Room-temperature spin valve effects in La$_{0.67}$Sr$_{0.33}$MnO$_3$/Alq$_3$/Co devices

S. Wang, Y.J. Shi, L. Lin, B.B. Chen, F.J. Yue, J. Du, H.F. Ding, F.M. Zhang, D. Wu*

National Laboratory of Solid State Microstructures and Department of Physics, Nanjing University, 22 Hankou Road, Nanjing 210093, China

ARTICLE INFO

ABSTRACT

We report room-temperature spin valve effects in Alq$_3$-based vertical organic spin valve (OSV) devices with direct interfaces between Alq$_3$ and the bottom and top ferromagnetic electrodes. In contrast to conventional OSVs, where the top electrode is directly deposited on top of organic layer, we use indirect deposition method. We find this method can significantly suppress the penetration of Co atoms into Alq$_3$ layer during deposition process, which is commonly found in conventional OSVs. The improved Alq$_3$/Co interface is further confirmed by comparing the magnetic moment of depositing Co onto Alq$_3$ and Si substrates by indirect and direct deposition methods. A penetration length of 12.5 nm in direct deposition Co on top of Alq$_3$ is estimated. And the demonstration of room-temperature spin valve effects indicates the improvement of spin injection efficiency at sharp Alq$_3$/Co interface.

1. Introduction

During last few years, there has been a considerable interest in studying the spin transport phenomena in organic materials owing to the expected long spin relaxation time and coherent length, originated from the weak spin–orbit coupling and hyperfine interaction in organic materials [1,2]. The conventional organic spin valves (OSVs) comprising two ferromagnetic electrodes separated by an organic spacer are the principal device structures to study the spin-dependent transport mechanism. In this device geometry, normally, the top ferromagnetic electrodes are directly deposited on top of the organic layer. The vaporized ferromagnetic atoms have high kinetic energy, which can lead to the penetration or diffusion of ferromagnetic atoms/clusters into organic layer and form the so-called ill-defined layer, resulting in short circuit in OSVs with thin organic layer. And the radiation of the deposition source can significantly heat up the substrates to facilitate atom penetration process. For example, an ill-defined layer of tris-(8, hydroxyquinoline) aluminum (Alq$_3$), caused by directly depositing Co, was estimated to be more than 50 nm based on measurement of transmission electron microscopy (TEM) combined with electron energy loss spectroscopy (EELS) [3]. Therefore, the occurrence of electrical short circuits in OSVs made with an Alq$_3$ layer of less than 100 nm thick was frequently observed [3–6].

This ferromagnetic atom penetration effects lead to the difficulties in fabricating reliable and reproducible OSVs and have been recognized as one of the main factors to hinder the study of

organic spintronics. To overcome this contacting problem, there are two approaches reported. One is the preparation of a thin insulating barrier, such as Al$_2$O$_3$ [7,8] and LiF [9], on the organic spacer before depositing top ferromagnetic electrode, which can protect the ferromagnetic atoms from directly depositing on organic layer. With this method a sharp interface can be achieved, the spin injection mechanism, however, is entirely different from metal/organic interface [9]. The other approach, which is called buffer layer assisted growth (BLAG), utilizes the fact that nanodots have much less penetration depth in organic layer than atoms [10]. The vaporized atoms form nanodots on the Xe buffer layer, which is condensed on the organic layer at low temperature before evaporation. The nanodot layer lands on the organic layer so as to suppress the penetration while desorption buffer layer by warming-up the samples. However, the influence of organic layer in depositing top electrodes cannot be completely excluded, particularly for thin organic spacer [10].

In recent years a deposition method called indirect deposition (ID) was successfully demonstrated to eliminate metal penetration through self-assembled monolayer molecules and showed reliable molecular junction devices [11,12]. The key of this method is to introduce an inert gas into the evaporation chamber during the top electrode deposition. The vaporized high temperature atoms collide with the inert gas several times, release their energies and "softly" land on molecular layer. In this work we adopt ID method to deposit Co onto Alq$_3$ layer to fabricate OSV devices. This approach shows the distinct suppression of Co penetration into Alq$_3$ layer and produces abrupt Alq$_3$/Co interfaces. We observe distinct spin-valve effects and obtain a high throughput production of devices using this method, indicating ID is a suitable approach to fabricate OSVs.

* Corresponding author.
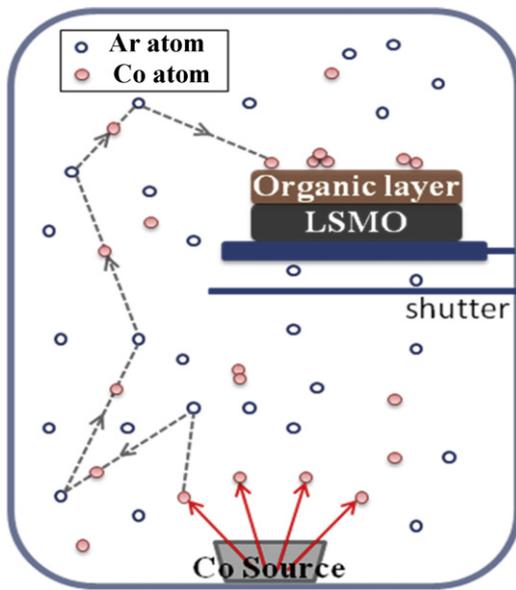 *E-mail address:* dwu@nju.edu.cn (D. Wu).

Fig. 1. Schematic diagram of the indirect deposition.

2. Experimental

About 100 nm thick $La_{0.7}Sr_{0.3}MnO_3$ (LSMO) films were epitaxially grown on $SrTiO_3(0\,0\,1)$ substrates by pulsed laser deposition. Prior to vacuum deposition of organic materials, the LSMO films were patterned by a lithographic process to define proper size. The Alq_3 films were deposited on LSMO at room temperature by thermal evaporation with a deposition rate of $\sim$0.07 nm/s. After that, the LSMO/Alq_3 bilayers were covered with a shadow mask and transferred into the e-beam evaporation chamber without breaking vacuum. To avoid the direct irradiation from deposition source to heat up the samples, a shutter was inserted between the sample holder and the source, as schematically illustrated in Fig. 1. Then the chamber was purged with Ar gas to a pressure of 3×10^{-3} Torr from a base pressure of $<2 \times 10^{-7}$ Torr before the deposition of the top Co electrodes. The Co atoms were evaporated by electron beam evaporation. In particular, the samples faced away from the Co source. As a result, only the Co atoms or clusters that scattered off the Ar gas atoms several times to reduce the kinetic energy to about room temperature (25 meV) would reach organic layer surface, comparing with kinetic energy of >100 meV for thermal deposition and a few eV for sputtering deposition. In this way the Co atom penetration into the organic layer should be dramatically suppressed. The deposition rate measured by a thickness monitor, which was beside the sample holder and faced the source, was about 0.01 nm/s. The effective deposition rates and Co thickness on organic layer were calibrated to be about 0.004 nm/s and 20 nm, respectively. Finally, the OSV devices, LSMO/Alq_3/Co, were turned back to face the source to directly deposit Al of 50 nm thick to cover the top Co electrodes at a rate of 0.03 nm/s. For comparison, we also fabricated LSMO/Alq_3/Co devices by directly depositing Co top electrodes with same Alq_3 thickness. The obtained device area is about 1×1 mm^2.

3. Results and discussion

In this work we choose the thickness of Alq_3 in the range of 35–40 nm, which is beyond the tunneling regime [13] but in the ill-define regime [3–6]. The typical spin-valve magnetoresistance (MR) curves for 40 nm thick Alq_3 measured with a bias voltage of 2 mV at 100 K and 300 K are shown in Fig. 2(a) and (b), respectively. The MR ratio is defined as $\Delta R/R_P = (R_{AP} - R_P)/R_P$, where R_{AP}
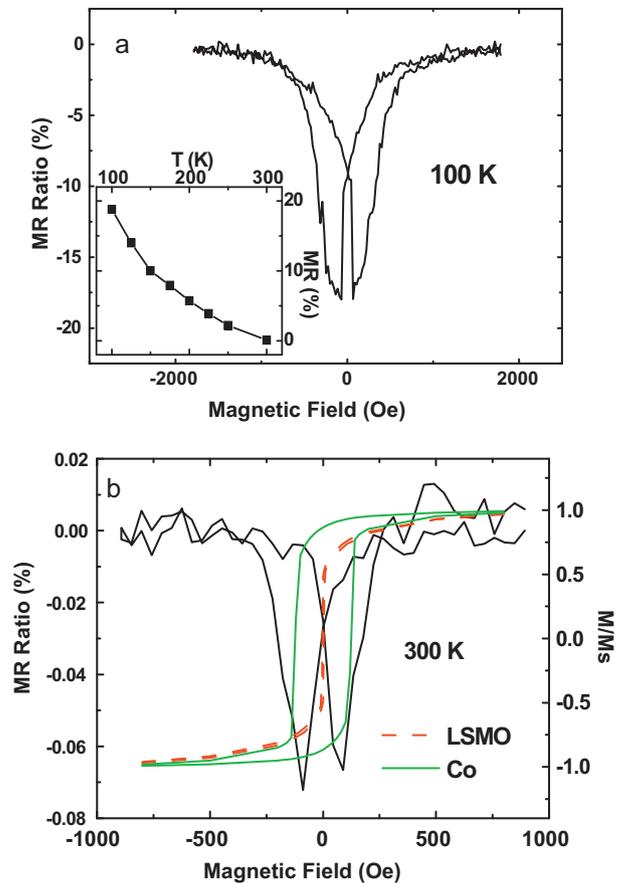

Fig. 2. (a) Magnetoresistance (MR) measured at 100 K with a 2 mV bias for OSVs with 40 nm Alq_3. The inset shows the temperature dependence of MR. (b) MR (black line) is measured at 300 K with a 2 mV bias. The magnetic hysteresis loops of LSMO film (red dot line) and indirectly deposited Co film on 500 nm thick Alq_3 (green line) are measured by VSM at room temperature for the same film thicknesses as used in the OSVs. (For interpretation of the references to color in this figure legend, the reader is referred to the web version of the article.)

and R_P denote the resistance for the magnetization of LSMO and Co in the antiparallel and parallel configurations, respectively. The magnetic hysteresis loops of LSMO film and indirectly deposited Co film on Alq_3 are measured by vibration sample magnetometer (VSM) at room temperature for the same film thicknesses as used in the OSVs, shown in the same plot of Fig. 2(b). Obviously, the coercivity of the LSMO and Co films corresponds to two switching fields in MR curve, indicating the realization of the parallel and antiparallel configurations for two ferromagnetic electrodes. We note that all LSMO/Alq_3/Co devices fabricated by ID exhibit an inverse spin-valve effect, $R_{AP} < R_P$, consistent with previous reports [4,7,10], suggesting that the positive MR observed in direct depositing Co electrode is probably due to the Co inclusions which may have different magnetic behavior from the films [3].

With the improved Co/Alq_3 interface, we observe a weak MR effect of 0.07% at room temperature, representing the possibility to apply spintronics in organic devices at room temperature. This value is comparable to a previous report of the OSV with Al_2O_3 inserted between Co and Alq_3 [7]. Although a measurable spin-valve effect is obtained at room temperature, the decrease of MR value with increasing temperature is much faster than that of magnetization of LSMO, of which Curie temperature is about 350 K, shown in the inset of Fig. 2(a), ruling out the possibility that the temperature dependence is due to lower Curie temperature of the Co inclusions in conventional OSVs.
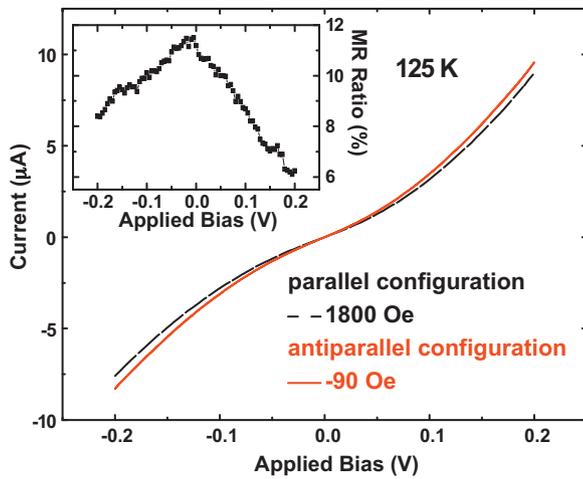
Fig. 3. I–V curves for LSMO and Co in antiparallel and parallel configurations at 125 K, respectively. The inset is the corresponding MR bias dependence calculated from the I–V curves.

Fig. 3 displays the current (I)–voltage (V) characteristics for two ferromagnetic electrodes in both antiparallel and parallel configurations measured at 125 K for the OSVs with 40 nm Alq_3. The I–V curves show weak non-linear behaviors, indicating the lack of pinholes. The resistance of our OSV is typically more than 10 kΩ. In contrast, the control devices with the same Alq_3 thickness fabricated by direct depositing Co electrodes always exhibit linear I–V curves and the resistance is two orders of magnitude smaller than that of devices fabricated by ID, which is a strong evidence of the relatively weak penetration of Co atoms into Alq_3 using ID. Owing to the stableness of the devices, the corresponding MR bias dependence can be calculated from the I–V curves, which is shown in the inset of Fig. 3. It has a strong asymmetry with respect to the voltage polarity, where the positive bias is defined as the current flowing from LSMO to Alq_3 and negative bias is from Co to Alq_3, with a maximum value at zero bias, in agreement with previous reports [4,14].

If the Co atoms penetrate or diffuse into the Alq_3 layer, a reduced magnetic moment of the Co films is expected due to the enhanced chemical reaction between Co and Alq_3 [15,16] and small Co clusters formed in the Alq_3 layer [3,4] which may not contribute to the magnetic moment at elevated temperature. Indeed, a magnetic dead layer was observed at ferromagnetic electrode/Alq_3 interface by polarized neutron reflectometry [17] and Co deposited on pentacene [18]. Therefore, in order to further confirm that the sharp interface between Co and Alq_3 is obtained by ID, we compare the magnetic moments of Co films on Alq_3 (500 nm)/Si(0 0 1) and Si(0 0 1) substrate by ID and control samples deposited by direct deposition. To minimize thickness variations, ~0.5 nm thick Co films were deposited simultaneously onto both Alq_3 and Si in each deposition method. An Alq_3 capping layer of 500 nm was grown after Co deposition. Fig. 4(a) and (b) show the hysteresis loops measured by VSM at room temperature for directly and indirectly depositing Co films onto Alq_3 and Si, respectively. We find that for direct deposition, the magnetic moment of Co on Alq_3 is 27 μemu/cm^2, corresponding to 1.7×10^{15} atoms/cm^2, smaller than that on Si due to the penetration of Co into Alq_3. In contrast, for ID, the magnetic moment of Co is almost the same on Alq_3 and Si. This result implies that the penetration of Co into Alq_3 is significantly suppressed in ID. If we assume that the Co atoms in Alq_3 layer completely lose magnetic moment and the area density of Co at the interface of Alq_3 side is equal to area density of Alq_3, which is about 1×10^{14} cm^{-2} based on an average lattice constant of Alq_3 crystals of 1 nm [19], a penetration length is estimated to be about
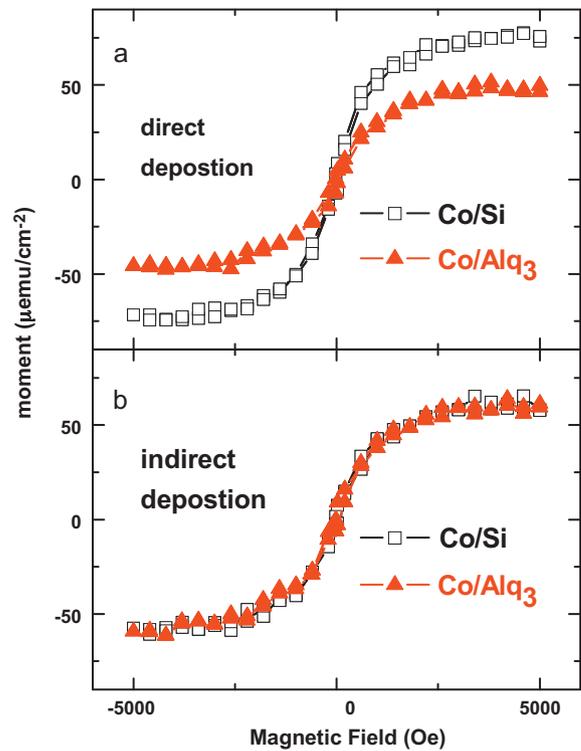

Fig. 4. (a) The hysteresis loops measured by VSM at room temperature for directly depositing Co films on Alq_3 and Si, respectively. (b) The hysteresis loops at room temperature for indirectly depositing Co films on Alq_3 and Si, respectively.

12.5 nm in exponential decay assumption, which agrees with an earlier report [3]. According to the ill-define thickness of ~100 nm [4–6], 3×10^{10} cm^{-2} Co atoms in Alq_3 can lead to short circuits.

4. Conclusions

In summary, we have developed a new method, ID, to fabricate high quality, reproducible OSV devices owing to the reduction of the penetration of the evaporated ferromagnetic atoms into the organic layers. The method relies on the scattering of the evaporated metallic atoms with inert gas to reduce kinetic energy, to deposit the ferromagnetic electrode Co on top of the organic layer Alq_3. We demonstrate that the ID approach can strongly suppress the diffusion between top ferromagnetic electrode and organic layer. The improvement of the Co/Alq_3 interface has led to spin-valve effect of 0.07% at room temperature. Our results indicate that ID is a promising method for the reliable fabrication of OSV devices.

References

[1] W.J.M. Naber, S. Faez, W.G. van der Wiel, J. Phys. D: Appl. Phys. 40 (2007) R205.
[2] V. Dediu, L. Hueso, I. Bergenti, C. Taliani, Nat. Mater. 8 (2009) 707.
[3] H. Vinzelberg, J. Schumann, D. Elefant, R.B. Gangineni, J. Thomas, B. Büchner, J. Appl. Phys. 103 (2008) 093720.
[4] Z.H. Xiong, D. Wu, Z.V. Vardeny, J. Shi, Nature (London) 427 (2004) 821.
[5] J.S. Jiang, J.E. Pearson, S.D. Bader, Phys. Rev. B 77 (2008) 035303.

[6] F.J. Wang, Z.H. Xiong, D. Wu, J. Shi, Z.V. Vardeny, Synth. Met. 155 (2005) 172.
[7] V. Dediu, L.E. Hueso, I. Bergenti, A. Riminucci, F. Borgatti, P. Graziosi, C. Newby, F. Casoli, M.P. De Jong, C. Taliani, Y. Zhan, Phys. Rev. B 78 (2008) 115203.
[8] T.S. Santos, J.S. Lee, P. Migdal, I.C. Lekshmi, B. Satpati, J.S. Moodera, Phys. Rev. Lett. 98 (2007) 016601.
[9] L. Schulz, L. Nuccio, M. Willis, P. Desai, P. Shakya, T. Kreouzis, V.K. Malik, C. Bernhard, F.L. Pratt, N.A. Morley, A. Suter, G.J. Nieuwenhuys, T. Prokscha, E. Morenzoni, W.P. Gillin, A.J. Drew, Nat. Mater. 10 (2011) 39.
[10] D. Sun, L. Yin, C. Sun, H. Guo, Z. Gai, X.-G. Zhang, T.Z. Ward, Z. Cheng, J. Shen, Phys. Rev. Lett. 104 (2010) 236602.
[11] T. Xu, I.R. Peterson, M.V. Lakshmikantham, R.M. Metzger, Angew. Chem. Int. Ed. 40 (2001) 1749.
[12] H. Haick, M. Ambrico, J. Ghabboun, T. Ligonzo, D. Cahen, Phys. Chem. Chem. Phys. 6 (2004) 4538.
[13] R. Lin, F. Wang, J. Rybicki, M. Wohlgenannt, K.A. Hutchinson, Phys. Rev. B 81 (2010) 195214.
[14] F.J. Wang, C.G. Yang, Z.V. Vardeny, Phys. Rev. B 75 (2007) 245324.
[15] Y.Q. Zhan, M.P. de Jong, F.H. Li, V. Dediu, M. Fahlman, W.R. Salaneck, Phys. Rev. B 78 (2008) 045208.
[16] W. Xu, J. Brauer, G. Szulczewski, M.S. Driver, A.N. Caruso, Appl. Phys. Lett. 94 (2009) 233302.
[17] Y. Liu, S.M. Watson, T. Lee, J.M. Gorham, H.E. Katz, J.A. Borchers, H.D. Fairbrother, D.H. Reich, Phys. Rev. B 79 (2009) 075312.
[18] Y. Hsu, Y. Hung, Y. Lin, Y. Lai, H. Chang, C. Wang, Y.L. Chan, C. Hsia, M. Luo, C. Lee, D.H. Wei, Synth. Met. 161 (2011) 575.
[19] M. Brinkmann, G. Gadret, M. Muccini, C. Taliani, N. Masciocchi, A. Sironi, J. Am. Chem. Soc. 122 (2000) 5147.